

Using LISA-like Gravitational Wave Detectors to Search for Primordial Black Holes

Huai-Ke Guo,¹ Jing Shu,^{1,2,3} and Yue Zhao^{4,5}

¹ CAS Key Laboratory of Theoretical Physics, Institute of Theoretical Physics,
Chinese Academy of Sciences, Beijing 100190, China

² School of Physical Sciences, University of Chinese Academy of Sciences, Beijing 100190, P. R. China

³ CAS Center for Excellence in Particle Physics, Beijing 100049, China

⁴ Tsung-Dao Lee Institute, and Department of Physics and Astronomy,
Shanghai Jiao Tong University, Shanghai 200240

⁵ Michigan Center for Theoretical Physics, University of Michigan, Ann Arbor, MI 48109

Primordial black holes (PBH), which can be naturally produced in the early universe, remain a promising dark matter candidate. They can merge with a supermassive black hole (SMBH) in the center of a galaxy and generate a gravitational wave (GW) signal in the favored frequency region of LISA-like experiments. In this work, we initiate the study of the event rate calculation for such extreme mass ratio inspirals (EMRI). Including the sensitivities of various proposed GW detectors, we find that such experiments offer a novel and outstanding tool to test the scenario where PBHs constitute (fraction of) dark matter. The PBH energy density fraction of DM (f_{PBH}) could potentially be explored for values as small as $10^{-3} \sim 10^{-4}$. Further, LISA has the capability to search for PBH masses up to $10^{-2} \sim 10^{-1} M_{\odot}$. Other proposed GW experiments can probe lower PBH mass regimes.

Introduction. Dark matter (DM) comprises about 27% of the energy density in our current universe [1]. However the identity of DM remains a mystery. It may be particles beyond the Standard Model, where popular choices are Weakly Interacting Massive Particle and axion. Primordial black holes (PBH) are also a promising candidate with a wide allowed mass range (for a PBH review, please see e.g. [2]). There have been a lot of efforts to study the fraction of DM as PBH, e.g. using gravitational lensing [3–11], the CMB temperature anisotropies and polarizations [12, 13], etc. The validity as well as astrophysical uncertainties of these constraints are still under debate, [14, 15] and thus it is interesting to explore this possibility through new and independent measurements.

The detection of the gravitational wave (GW) events from black hole binaries by the LIGO and Virgo collaborations [16–18] has begun the era of GW astronomy. GW observations provide a novel method to study the universe. Many GW detectors have been proposed (see Ref [19] for a review). In particular, Laser Interferometer Space Antenna (LISA), which aims for a much lower frequency regime than that of LIGO-like ground-based detectors, has been approved recently [20]. One major scientific goal of LISA is to measure the GW produced by the merger of a SMBH and a compact object (CO), such as a neutron star, white dwarf or stellar BH. In such EMRIs [21], GW frequencies typically range from 10^{-4} to 1 Hz for SMBH masses between $10^4 M_{\odot}$ and $10^7 M_{\odot}$. Once such events are observed, the intrinsic parameters of the binary system can be measured in high precision [22] due to the long-lasting inspiral process before merging.

Aside from their significant impacts for astronomy, the observation of GWs may also open a new avenue to study the possibility of PBHs playing the role of DM.

Especially, Ref. [23–29] study the interesting question of whether the BHs detected by LIGO can be PBHs which form a non-trivial fraction of DM. Using LIGO and LISA to probe extremely small mass PBH is studied in [30]. For PBHs with mass of $\mathcal{O}(10) M_{\odot}$, it is hard to distinguish them from stellar BHs. However, LIGO is not ideal to probe other PBH mass ranges, either due to the shifted frequency region or reduced magnitude of GW radiation. On the other hand, the mergers between PBHs and SMBHs produce GWs in the favored frequency regions of LISA-like experiments. Such frequencies are mainly determined by SMBH mass and are independent of PBH mass. This indicates that, unlike LIGO, we potentially have the access to a vast mass range of PBHs, which lies outside the mass window of astrophysical COs. Therefore, observation of these events may be used to claim the discovery of PBHs. Moreover, the DM profile peaks at the center of a galaxy, indicating the possibility of a large number density of PBHs in the neighborhood of a SMBH. This may induce a significant EMRI rate caused by PBH-SMBH mergers.

In this letter, we carry out the first study of the event rate estimation for PBH-SMBH mergers, taking into considerations the sensitivities of different experiments. In the next section, we outline the essential ingredients for the calculation. Then we calculate each of them in the later sections. After that, we put everything together and interpret the observable event rate for different experiments as their capabilities to probe PBH-as-DM scenarios. We find these experiments provide us a powerful tool to study a large unexplored parameter space. Not only could the sensitivity to f_{PBH} be as good as $10^{-3} \sim 10^{-4}$, but also the lower limit of PBH masses that can be probed is potentially far from the astrophysical CO mass region. This could be used to discover PBH

from these GW experiments.

Ingredients for EMRI Rate Calculation. EMRI has been carefully studied in the context of astrophysics. In particular, the merger rate between SMBH and astrophysical COs has been calculated. Let us first summarize the key ingredients in this calculation.

The event rate observed by a GW detector can be written as,

$$\Gamma = \int \mathcal{R}(M, \mu) \left(\frac{dn(M, z)}{dM} dM \right) (p(s, z) ds) \left(\frac{dV_c}{dz} dz \right), \quad (1)$$

where $\mathcal{R}(M, \mu)$ is the intrinsic EMRI rate in a galaxy hosting a SMBH with mass M . The mass of the CO is μ . The $dn(M, z)/dM$ and $p(s, z)$ are the mass spectrum and spin, s , distribution of SMBHs. They are functions of redshift z due to the evolution of galaxies. If one only focuses on late times, z -dependence may be approximately removed. From the popIII model [31], most of the SMBHs within the LISA range, i.e. with mass comparable or smaller than $10^7 M_\odot$, are expected to have near maximal spins [32]. Further, EMRI rates are calculated with various spin distributions, and the difference appears to be less than 10%. Thus in the following discussion, we fix $s = 0.999$.

In addition $(\frac{dV_c}{dz} dz)$ is the comoving volume integral as a function of z . Since the GW strength decreases when distance increases, not all EMRI events are detectable by a GW detector. Thus the sensitivity of an experiment imposes a maximum z , z_{max} , as a function of (M, s, μ) , the details of which we will discuss in later sections.

Among these ingredients, the most non-trivial is $\mathcal{R}(M, \mu)$. The intrinsic EMRI rate can be calculated by solving the Fokker-Planck equation, which describes the diffusion of the CO distribution functions. The result is a function of the mass and density of the CO. Although the precise result has yet to be obtained by numerical calculations, qualitative estimation is possible and agrees well with numerics [33].

As far as is known, the detailed numerical calculation on \mathcal{R} is only done assuming COs are white dwarfs, neutron stars and stellar BHs. It is important to derive a reasonable estimation on intrinsic EMRI rate for PBHs whose mass and number density are dramatically different from those of astrophysical COs. We will follow the analysis in [33] and present an analytical formula to scale \mathcal{R} for stellar BHs as a function of the PBH's properties.

In the next few sections, we prepare the ingredients for the calculation of Eq.(1). We first discuss the DM profile, which determines the number density of PBHs near a SMBH. Astrophysical empirical equations are applied to relate DM profiles to SMBH masses. Then we review the calculation of the GW strain from EMRIs. We show sensitivities of various GW detectors and discuss the calculation of signal-to-noise-ratio (SNR). We also consider the subtlety of how detector operation time affects the

SNR estimation. After that, we present a detailed analysis of how the intrinsic EMRI rate scales as a function of PBH number density and mass. Last, we put everything together to study the event rate for various GW detectors.

Dark Matter Halo Profile. The PBH-SMBH merger rate highly depends on the number density of PBHs around SMBH. EMRIs are mainly produced by COs within the radius of influence of the SMBH [34],

$$r_h = \frac{GM}{\sigma^2} = 2\text{pc} \left(\frac{M}{3 \times 10^6 M_\odot} \right)^{1/2}, \quad (2)$$

where σ is the velocity dispersion in the bulge, and the following $M - \sigma$ relation [35–37] is applied:

$$M = 10^8 M_\odot \left(\frac{\sigma}{200\text{km/s}} \right)^4. \quad (3)$$

Since r_h is $\mathcal{O}(\text{pc})$, the EMRI rate is sensitive to the DM energy density in the innermost region. While collisionless N-body simulations of cold DM indicate a cuspy profile [38–41], a cored profile may be obtained if other effects, such as baryonic feedback, are taken into consideration [42]. On the other hand, assuming adiabatic growth of SMBHs, a spike around the galactic center can be induced [43, 44] and is more pronounced for a Kerr SMBH [45]. Especially, in [29], a spike connected to the NFW profile is used to study the PBH-PBH merger rate, which is enhanced as expected. In this letter, we only use the NFW profile [39, 40] as an illustration and note that cored (spiky) profiles may lead to smaller (larger) rates.

The NFW profile can be parametrized as

$$\rho(r) = \frac{\rho_s}{\frac{r}{R_s} (1 + \frac{r}{R_s})^2}, \quad (4)$$

where ρ_s and R_s are the characteristic density and scale radius, respectively. The enclosed mass within a radius R (equivalently, the dimensionless radius $c \equiv R/R_s$) is

$$m_{\text{Halo}} = \int_0^{R_{\text{max}}} 4\pi r^2 \rho(r) dr = 4\pi \rho_s R_s^3 g(c_{\text{max}}), \quad (5)$$

where the function $g(x) = \ln(1+x) - x/(1+x)$ is defined for later convenience. Since m_{Halo} diverges, a cutoff radius is conventionally defined such that the enclosed average DM energy density is 200 times the critical density of the universe ρ_c . The DM halo profile can then be specified by the two parameters c_{200} and M_{200} , where M_{200} is the enclosed DM halo mass, and c_{200} is the corresponding radius in units of R_s :

$$\rho_s = \frac{200}{3} \frac{c_{200}^3}{g(c_{200})} \rho_c; \quad R_s = \left[\frac{M_{200}}{4\pi \rho_s g(c_{200})} \right]^{1/3}. \quad (6)$$

Further, at late times in the universe, i.e. at small redshift, c_{200} and M_{200} can be related through the

concentration-mass relation [46],

$$c_{200} = 10^{0.905} \left(\frac{M_{200}}{10^{12} h^{-1} M_{\odot}} \right)^{-0.101}. \quad (7)$$

Here $h = 0.673$ is the Hubble parameter at present time. The DM halo can then be specified by a single parameter, chosen here as M_{200} . Since Eq. (7) only holds at small z , we truncate the spatial integral in the rate calculation at a maximal distance. More explicitly, we take $z \leq 1$ ($r_0 \leq 3.5 \text{Gpc}$).

Last, we need the connection between the halo mass M_{200} and the SMBH mass M . This is given in [47],

$$\frac{M}{3 \times 10^6 M_{\odot}} \approx 3.3 \left(\frac{M_{200}}{10^{12} M_{\odot}} \right)^{1.65}. \quad (8)$$

Therefore, the DM halo profile can be expressed as a simple function of the SMBH mass. We note that the total DM mass within r_h , according to the above NFW profile, is $\sim 10^{-2}$ of the SMBH mass. Thus the existence of DM can be treated as small perturbation.

Gravitational Wave Strain and SNR. Modeling GW emission from an EMRI system is non-trivial. Several formalisms have been studied. For example, the numerical-kludge model [48, 49] is more accurate but computationally expensive. The analytic kludge model (AK) [22, 50], on the other hand, is cheaper but at the price of accuracy. Within AK formalism, the two ways to truncate the calculation are labeled as AKK and AKS, which tend to give optimistic/conservative estimates of SNR. These two choices characterize the uncertainties of the calculation. Last, gravitational wave emission can also be approximately calculated for circular and equatorial EMRIs by solving the Teukolsky equation [51–53]. This method is also used in [54] to estimate the EMRI rate for LISA. Although the orbits of EMRIs generically have moderate eccentricity and are inclined, the result consistently falls between those from AKK and AKS, as shown in [32].

In this letter, we adopt the result from [53] where the GW strain is organized into a set of harmonics $h_{c,m}(f)$ with m the harmonic number,

$$h_{c,1} = \frac{5}{\sqrt{672\pi}} \frac{\eta^{1/2} M}{r_o} \tilde{\Omega}^{1/6} \mathcal{H}_{c,1},$$

$$h_{c,m} = \sqrt{\frac{5(m+1)(m+2)(2m+1)! m^{2m}}{12\pi(m-1)[2^m m! (2m+1)!!]^2}} \frac{\eta^{1/2} M}{r_o} \times \tilde{\Omega}^{(2m-5)/6} \mathcal{H}_{c,m}, \quad m \geq 2. \quad (9)$$

The equations are in geometrized units ($G = 1$ and $c = 1$). Here η is the ratio of the inspiraling object mass μ and SMBH mass M , i.e. $\eta = \mu/M$. r_o is the distance from the merger to us. A dimensionless orbital angular velocity $\tilde{\Omega}$ is defined as $\tilde{\Omega} \equiv M\Omega = 1/(\tilde{r}^{3/2} + s)$ where $\tilde{r} \equiv r/M$ with r being the Boyer-Lindquist radial coordinates

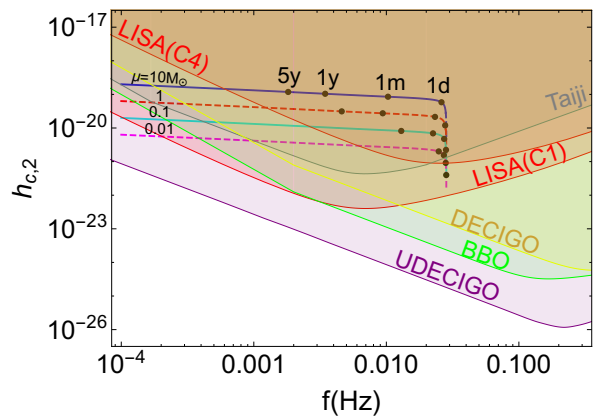


FIG. 1: The characteristic strain $h_{c,2}$ is plotted for different choices of PBH mass μ . The SMBH has mass and spin as $10^6 M_{\odot}$ and 0.999. The distance to the earth is taken to be 1Gpc. The dots indicate the remaining time before the merger. The sensitivities of various proposed experiments, $h_n(f)$, are also presented.

of the orbit. $\mathcal{H}_{c,m}$ is the relativistic correction and is provided in [53] with various choices of s and r .

The maximal frequency of GW radiation f_{\max} occurs at the innermost stable circular orbit (ISCO) at radius r_{ISCO} , which is a function of M and a [55]. In Fig. 1, we show $h_{c,2}$ with different choices of μ . The experimental sensitivity is quantified by $h_n(f_m) \equiv \sqrt{f S_n(f_m)}$, where $S_n(f_m)$ is the one-sided noise power spectral density [19]. Optimistic and pessimistic LISA configurations N2A5M5L6 (C1) and N1A1M2L4 (C4) [31] are presented [72]. We also include several other proposed experiments, i.e. Taiji GW project, Big Bang Observer (BBO), DECi-hertz Interferometer Gravitational wave Observatory (DECIGO) [19], and Ultimate-DECIGO (UDE-CIGO) [56].

It is instructive to make a qualitative comparison between LISA and LIGO at this point. While LISA and LIGO have their best sensitivities at different frequency regimes, h_n of LISA and LIGO are at a similar order of magnitude. Around r_{ISCO} , h_c scales as $\sqrt{\mu M}$. The events observed by LIGO have masses as $\mathcal{O}(10) M_{\odot}$. At the same distance, a similar order of magnitude of h_c can be achieved if $\mu \sim 10^{-3} M_{\odot}$ when $M \sim 10^6 M_{\odot}$. This indicates the possibility for LISA-like GW detectors to probe light PBHs.

A GW signal can be detected only if the SNR is above a certain threshold. The SNR can be calculated as

$$\text{SNR}^2 = \frac{\mathcal{S}^2}{\mathcal{N}^2} = \sum_m \int \left[\frac{h_{c,m}(f_m)}{h_n(f_m)} \right]^2 d \ln f_m, \quad (10)$$

where \mathcal{S} and \mathcal{N} are the signal and noise obtained with matched-filtering [19]. A widely adopted choice of threshold is $\text{SNR} \geq 15$.

One subtlety appears when calculating SNR. While the slow inspirals may last for a very long time, e.g. $\mathcal{O}(\text{Gyr})$,

LISA-like GW detectors can only operate at timescales $\mathcal{O}(\text{yr})$. The GW frequency increases during inspiral and achieves its maximal value f_{max} when $r \sim r_{\text{ISCO}}$, after which the inspiral stops and the plunge occurs. Only a finite frequency window near the maximal frequency can be recorded during the operation time of an experiment. A truncation needs to be imposed accordingly for the integration range in Eq.(10). This can be calculated by the total time remaining before the plunge [53, 57]

$$T = \frac{5}{256} \frac{1}{\mu} \frac{M^2}{\bar{\Omega}^{8/3}} \mathcal{T}, \quad (11)$$

where \mathcal{T} is the general relativistic correction with details listed in [53]. Since we are focused on the merger events, setting T to the operation time gives the lower bound of the frequency integral f_{min} . Note for smaller PBH masses, the integration range can be very small since GW radiation power is lower for a lighter CO. Thus light PBHs linger around ISCO for a longer time and the frequency variation is tiny on timescales $\mathcal{O}(\text{yr})$. For light PBHs, the variation of frequency during $\mathcal{O}(\text{yr})$ is small. In this limit, $\Delta f/f \sim \mu/M^2$. Thus for a fixed μ , a lower M provides a larger integral range when calculating SNR.

For each EMRI, the SNR imposes an upper limit on redshift. Combined with the truncation imposed in the previous section, the limit of the spatial integral is determined by $z_{\text{max}} = \min(z|_{\text{SNR}=15}, 1)$.

Intrinsic EMRI Rate for PBH-SMBH. A CO can change its orbit in two ways: *i*) gravitationally scattering with another CO object, or *ii*) losing energy by GW radiation. If gravitational scattering brings a CO to an orbit direct falling into a SMBH, this plunge will not produce a GW observable by LISA-like detectors. On the other hand, if a SMBH-CO merger is induced by GW radiation after many orbits, this results in a slow inspiral which can be potentially detected. This will be our focus. [73]

The intrinsic EMRI rate induced by SMBH-stellar BH slow inspiral has been calculated using the Fokker-Planck equation in [58–60]. The stellar BH mass is set to be $10M_{\odot}$, and the number density is taken to be 0.1% of the total number density of astrophysical objects within r_h . It can be explicitly written as [60]

$$n_{\text{BH}} = 40 \text{ pc}^{-3} \left(\frac{M}{3 \times 10^6 M_{\odot}} \right)^{-1/2}. \quad (12)$$

The intrinsic EMRI rate of such system scales with M as [54, 60]

$$\mathcal{R}_{\text{astro}}(M) = 400 \text{Gyr}^{-1} \left(\frac{M}{3 \times 10^6 M_{\odot}} \right)^{-0.15}. \quad (13)$$

Now we study how Eq.(13) scales as a function of PBH number density and mass.

First, we rescale the number density of PBHs with respect to that of stellar BHs in Eq. (12),

$$\mathcal{G}(M, \mu) = f_{\text{PBH}} \frac{\rho_{\text{NFW}}(M, r_h(M))/\mu}{n_{\text{BH}}(M)}. \quad (14)$$

For example, when $\mu = 10M_{\odot}$ and $M = 10^6 M_{\odot}$, \mathcal{G} is $\mathcal{O}(1)$.

The timescale that brings a PBH to an orbit of slow inspiral can be written as a function of relaxation time t_h at r_h . According to [61], for generic astrophysical objects, the relaxation time is determined by the species with largest $m_i^2 n_i$ where m_i and n_i are the mass and number density of each species. Using the NFW profile, the total mass of the PBH within r_h is only a small fraction. Given the parameter choice in [60], the relaxation of PBHs is mainly controlled by their scattering with main-sequence stars (MS). Accordingly we expect t_h is approximately independent of PBH mass.

The angular momentum relaxation time can be written as

$$t_J(J, a) = t_h \left[\frac{J}{J_m(a)} \right]^2 \left(\frac{a}{r_h} \right)^p. \quad (15)$$

Here a is the semi-major axis of an orbit, and $J_m(a) = \sqrt{Ma}$ is the maximal (circular) angular momentum for a specific energy. p is related to the spatial profile of the astrophysical objects which dominate the relaxation process of PBHs, i.e. $n_{\text{MS}} \sim r^{-3/2-p}$.

Now let us estimate the timescale of a slow inspiral. This process lasts a long time, much longer than the period of the orbit. The energy carried away by gravitational radiation per period is [33, 50]:

$$\Delta E = E_1 \left(\frac{J}{J_{lc}} \right)^{-7} \quad (16)$$

with

$$E_1 = \frac{85\pi}{3 \times 2^{13}} \frac{\mu}{M}; \quad J_{lc} = 4M. \quad (17)$$

Note the energy and angular momentum are defined in units of PBH mass μ .

For an orbit with high eccentricity, periapse approximately remains a constant, and the time for a CO with initial specific energy ϵ_0 to finish the inspiral is

$$t_0 = \int_{\epsilon_0}^{\infty} \frac{d\epsilon}{d\epsilon/dt} \approx \frac{2\pi\sqrt{Ma}}{\Delta E} \sim \mu^{-1}. \quad (18)$$

Here we only pay attention to its dependence on μ since the goal is to estimate the intrinsic EMRI rate by rescaling Eq.(13)

It is important to ensure that the slow inspiral can continue without being disrupted by further scatterings. A critical value of a is defined by the ratio of t_0 and t_J , i.e.

$t_0(J_{lc}, a_c)/t_J(J_{lc}, a_c) = 1$. For an orbit with $a < a_c$, a CO has a large chance to fall into SMBH without disruptions. This critical value a_c is given by,

$$\frac{a_c}{r_h} = \left(\frac{d_c}{r_h}\right)^{\frac{3}{3-2p}}; \quad d_c = \left(\frac{8\sqrt{M}E_1 t_h}{\pi}\right)^{2/3}. \quad (19)$$

Using the analytic solution of the Fokker-Planck equation in [33], one obtains an estimation of the intrinsic EMRI rate for PBHs with arbitrary mass,

$$\begin{aligned} \mathcal{R}_{\text{PBH}}(M, \mu) &= \int_0^{a_c} \frac{da n_{\text{PBH}}(a)}{\ln(J_m(a_c)/J_{lc})t_h} \left(\frac{r_h}{a}\right)^p \\ &\sim \frac{n_{\text{PBH}}(r_h)}{t_h \ln[J_m(a_c)/J_{lc}]} \left(\frac{a_c}{r_h}\right)^{3/2-2p} \\ &\sim \mathcal{G}(M, \mu) \mu^{\frac{4p-3}{2p-3}} \mathcal{R}_{\text{astro}}(M). \end{aligned} \quad (20)$$

where $n_{\text{PBH}}(a)$ is the PBH number density at a [74].

As shown in Eq.(20), the intrinsic EMRI rate is sensitive to the choice of p , which ranges from 0 to 0.25 [59, 62–64]. To show its effects qualitatively, we present the results with different choices of p in the next section.

PBH Constraints. Finally, to estimate event rate, we take the mass spectrum of SMBHs given in Ref. [31, 32],

$$\frac{dn}{d \ln M} = 0.005 \left(\frac{M}{3 \times 10^6 M_\odot}\right)^{-0.3} \text{Mpc}^{-3}, \quad (21)$$

with the range of the SMBH masses taken to be $10^4 M_\odot \leq M \leq 10^7 M_\odot$. One can convert the expected observable PBH-SMBH EMRI rate into the sensitivity to PBH energy density fraction of DM, f_{PBH} .

Once such EMRI events are observed, the detailed waveform provides an excellent handle to extract information on the system [22, 32], and μ can be measured by analyzing the time-dependence of the orbit. The stellar BHs are expected to have masses ranging from 5 to few tens M_\odot [65]. If PBHs are within the same mass regime, e.g. motivated in [66], stellar BHs may behave as a background of the PBH search. Further, mergers between SMBH and other astrophysical COs, such as neutron stars and white dwarfs, may also contribute as PBH-SMBH background. The mass of white dwarfs (neutron stars) is unlikely to be smaller than $0.6 M_\odot$ ($1 M_\odot$). If PBHs are much lighter than those astrophysical COs, the background is free. In that case, one event observed is enough to declare discovery.

In Fig. 2, with various choices of GW detectors, we present the value of f_{PBH} which generate one PBH-SMBH EMRI with $\text{SNR} > 15$ during a 5-year operation of the experiment. The dark grey region starts at $3 M_\odot$ where stellar BHs begin to contribute as background. From $0.3 M_\odot$, white dwarfs and neutron stars become important. We stop our calculation at $\mu = 10^2 M_\odot$ so that EMRI remains a reasonable approximation, especially for

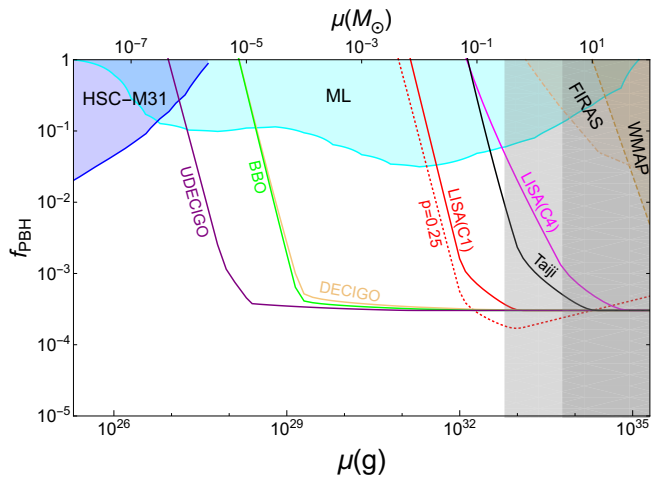


FIG. 2: We show the value of $f_{\text{PBH}}(\mu)$ which is expected to give one observable PBH-SMBH EMRI event during the 5-year mission of an experiment. Various detector configurations and sensitivities are considered. The solid lines are obtained by taking $p = 0$, and the dashed red line corresponds to the LISA C1 sensitivity with $p = 0.25$. The microlensing constraint, HSC-M31, is from Ref. [6], and other constraints are from Ref. [27]. The regions where $0.3 M_\odot < \mu < 3 M_\odot$ and $3 M_\odot < \mu < 100 M_\odot$ are shaded. Here the background from neutron star (white dwarf) [67, 68] and stellar BHs, respectively, needs to be carefully considered.

galaxies with light SMBHs ($10^4 M_\odot$). The existing constraints on f_{PBH} are included, and LISA-like GW experiments have good potential to probe the unexplored parameter space.

There are several important features of this sensitivity curve.

i). When μ is not too small, with a sufficiently sensitive GW detector, all EMRIs happening within $z = 1$ can be observed. As indicated in Eq. (20), the intrinsic EMRI rate $\mathcal{R}_{\text{PBH}}(M, \mu)$ is independent of μ when $p = 0$. This explains the flatness of f_{PBH} curves in the large μ regime. When lowering μ , not all EMRIs exceed the SNR threshold. This produces the turning point which is determined by the detector sensitivity.

ii). As discussed below Eq.(11), for a fixed μ , smaller M gives a larger integration range of $\Delta f/f$ in the calculation of SNR, i.e. $\Delta f/f \sim 1/M^2$. Although the gravitational wave strain scales as $h_c \sim \sqrt{M}$, a better SNR can still be achieved for lighter SMBH assuming h_n is the same. Given the SMBH mass distribution also increases when M decreases as shown in Eq.(21), this indicates that a GW experiment may have better sensitivity for lighter PBHs if its best frequency region is higher. This is why the reach of DECIGO is comparable to that of BBO even though its sensitivity is worse in lower frequency.

In Fig. 2, we also study the reach limit with a different choice of p , shown as the dashed curve for LISA(C1).

For $p \neq 0$, the dependence on μ becomes non-trivial for the intrinsic EMRI rate. When p is positive, the probed region is further extended in the lighter PBH region. As discussed above, p is related to the spatial distribution of the astrophysical objects, presumably MS, and controls the relaxation time. It also affects the EMRI rate of merging SMBHs and ordinary astrophysical COs, the observation of which can help to reduce the uncertainty in our PBH-SMBH rate calculation.

Discussion. In this letter, we explore the possibility of using LISA-like GW detectors to look for PBH-SMBH EMRI events. The frequency of the GWs is mainly determined by the mass of SMBH, and a vast range of PBH masses can be probed by such experiments. Especially, a BH much lighter than $0.3 M_{\odot}$ is not expected from astrophysics. The detection of such a SMBH-PBH merger outside the astrophysical CO mass window is potentially enough to declare the discovery of PBHs.

We find that LISA-like GW experiments provide a novel and promising way to test the scenario where PBHs are (a fraction of) DM. The sensitivity to f_{PBH} in certain mass regimes could be as good as $10^{-3} \sim 10^{-4}$, which is much better than the existing constraints.

Our analysis here initiates the study of PBHs as DM using LISA-like GW detectors which connects astronomy and GW and DM physics. We expect that our current results can be significantly improved with better knowledge from those interdisciplinary areas in the future. For example, we truncate our calculation at $z = 1$ due to the uncertain validity of astrophysical empirical relations, such as Eq.(7) at high redshift. With a better understanding of such a relation, the higher z region could be included, and a much smaller f_{PBH} may be explored. Furthermore, astrophysical uncertainties, such as mass and spin distributions of SMBHs, would affect the rate estimation. The observation of EMRI events induced by astrophysical COs also provides valuable information. This may have feedback to the PBH calculation and reduce the theoretical uncertainties.

As a final comment, as we discussed above, lighter SMBHs may potentially be more beneficial to search for small mass PBHs, both because of the higher number density from the SMBH mass spectrum as well as the larger integration window on frequency in the SNR calculation. This serves as a guideline for the optimization of a light PBH search in future LISA-like GW experiments.

Acknowledgement. We would like to thank Yanbei Chen, Runqiu Liu, Aaron Pierce, Tao Ren, Keith Riles and Ben Safdi for helpful discussions. Especially, we thank Xian Chen, Josh Foster for carefully reading our draft and giving valuable comments. JS is supported by the National Natural Science Foundation of China (NSFC) under grant No.11647601, No.11690022 and No.11675243 and also supported by the Strategic Priority

Research Program of the Chinese Academy of Sciences under grant No.XDB21010200 and No.XDB23030100. YZ thank the support of grant from the Office of Science and Technology, Shanghai Municipal Government (No. 16DZ2260200). YZ is also supported by US Department of Energy under grant de-sc0007859.

-
- [1] **Planck** Collaboration, P. A. R. Ade *et al.*, “Planck 2015 results. XIII. Cosmological parameters,” *Astron. Astrophys.* **594** (2016) A13, [arXiv:1502.01589 \[astro-ph.CO\]](#).
 - [2] B. J. Carr, K. Kohri, Y. Sendouda, and J. Yokoyama, “New cosmological constraints on primordial black holes,” *Phys. Rev.* **D81** (2010) 104019, [arXiv:0912.5297 \[astro-ph.CO\]](#).
 - [3] R. J. Nemiroff, G. F. Marani, J. P. Norris, and J. T. Bonnell, “Limits on the cosmological abundance of supermassive compact objects from a millilensing search in gamma-ray burst data,” *Phys. Rev. Lett.* **86** (2001) 580, [arXiv:astro-ph/0101488 \[astro-ph\]](#).
 - [4] J. J. Dalcanton, C. R. Canizares, A. Granados, C. C. Steidel, and J. T. Stocke, “Observational limits on Omega in stars, brown dwarfs, and stellar remnants from gravitational microlensing,”.
 - [5] P. N. Wilkinson, D. R. Henstock, I. W. A. Browne, A. G. Polatidis, P. Augusto, A. C. S. Readhead, T. J. Pearson, W. Xu, G. B. Taylor, and R. C. Vermeulen, “Limits on the cosmological abundance of supermassive compact objects from a search for multiple imaging in compact radio sources,” *Phys. Rev. Lett.* **86** (2001) 584–587, [arXiv:astro-ph/0101328 \[astro-ph\]](#).
 - [6] H. Niikura, M. Takada, N. Yasuda, R. H. Lupton, T. Sumi, S. More, A. More, M. Oguri, and M. Chiba, “Microlensing constraints on $10^{-10} M_{\odot}$ -scale primordial black holes from high-cadence observation of M31 with Hyper Suprime-Cam,” [arXiv:1701.02151 \[astro-ph.CO\]](#).
 - [7] **EROS-2** Collaboration, P. Tisserand *et al.*, “Limits on the Macho Content of the Galactic Halo from the EROS-2 Survey of the Magellanic Clouds,” *Astron. Astrophys.* **469** (2007) 387–404, [arXiv:astro-ph/0607207 \[astro-ph\]](#).
 - [8] L. Wyrzykowski *et al.*, “The OGLE View of Microlensing towards the Magellanic Clouds. IV. OGLE-III SMC Data and Final Conclusions on MACHOs,” *Mon. Not. Roy. Astron. Soc.* **416** (2011) 2949, [arXiv:1106.2925 \[astro-ph.GA\]](#).
 - [9] **Macho** Collaboration, R. A. Allsman *et al.*, “MACHO project limits on black hole dark matter in the 1-30 solar mass range,” *Astrophys. J.* **550** (2001) L169, [arXiv:astro-ph/0011506 \[astro-ph\]](#).
 - [10] **MACHO**, **EROS** Collaboration, C. Alcock *et al.*, “EROS and MACHO combined limits on planetary mass dark matter in the galactic halo,” *Astrophys. J.* **499** (1998) L9, [arXiv:astro-ph/9803082 \[astro-ph\]](#).
 - [11] K. Griest, A. M. Cieplak, and M. J. Lehner, “Experimental Limits on Primordial Black Hole Dark Matter from the First 2 yr of Kepler Data,” *Astrophys. J.* **786** no. 2, (2014) 158, [arXiv:1307.5798 \[astro-ph.CO\]](#).
 - [12] M. Ricotti, J. P. Ostriker, and K. J. Mack, “Effect of

- Primordial Black Holes on the Cosmic Microwave Background and Cosmological Parameter Estimates,” *Astrophys. J.* **680** (2008) 829, [arXiv:0709.0524 \[astro-ph\]](#).
- [13] L. Chen, Q.-G. Huang, and K. Wang, “Constraint on the abundance of primordial black holes in dark matter from Planck data,” *JCAP* **1612** no. 12, (2016) 044, [arXiv:1608.02174 \[astro-ph.CO\]](#).
- [14] Y. Ali-Hamoud and M. Kamionkowski, “Cosmic microwave background limits on accreting primordial black holes,” *Phys. Rev. D* **95** no. 4, (2017) 043534, [arXiv:1612.05644 \[astro-ph.CO\]](#).
- [15] A. M. Green, “Astrophysical uncertainties on stellar microlensing constraints on multi-Solar mass primordial black hole dark matter,” [arXiv:1705.10818 \[astro-ph.CO\]](#).
- [16] **Virgo, LIGO Scientific** Collaboration, B. P. Abbott *et al.*, “Observation of Gravitational Waves from a Binary Black Hole Merger,” *Phys. Rev. Lett.* **116** no. 6, (2016) 061102, [arXiv:1602.03837 \[gr-qc\]](#).
- [17] **Virgo, LIGO Scientific** Collaboration, B. P. Abbott *et al.*, “GW151226: Observation of Gravitational Waves from a 22-Solar-Mass Binary Black Hole Coalescence,” *Phys. Rev. Lett.* **116** no. 24, (2016) 241103, [arXiv:1606.04855 \[gr-qc\]](#).
- [18] **VIRGO, LIGO Scientific** Collaboration, B. P. Abbott *et al.*, “GW170104: Observation of a 50-Solar-Mass Binary Black Hole Coalescence at Redshift 0.2,” *Phys. Rev. Lett.* **118** no. 22, (2017) 221101, [arXiv:1706.01812 \[gr-qc\]](#).
- [19] C. J. Moore, R. H. Cole, and C. P. L. Berry, “Gravitational-wave sensitivity curves,” *Class. Quant. Grav.* **32** no. 1, (2015) 015014, [arXiv:1408.0740 \[gr-qc\]](#).
- [20] H. Audley *et al.*, “Laser Interferometer Space Antenna,” [arXiv:1702.00786 \[astro-ph.IM\]](#).
- [21] P. Amaro-Seoane, J. R. Gair, A. Pound, S. A. Hughes, and C. F. Sopuerta, “Research Update on Extreme-Mass-Ratio Inspirals,” *J. Phys. Conf. Ser.* **610** no. 1, (2015) 012002, [arXiv:1410.0958 \[astro-ph.CO\]](#).
- [22] L. Barack and C. Cutler, “LISA capture sources: Approximate waveforms, signal-to-noise ratios, and parameter estimation accuracy,” *Phys. Rev. D* **69** (2004) 082005, [arXiv:gr-qc/0310125 \[gr-qc\]](#).
- [23] S. Bird, I. Cholis, J. B. Muoz, Y. Ali-Hamoud, M. Kamionkowski, E. D. Kovetz, A. Raccanelli, and A. G. Riess, “Did LIGO detect dark matter?,” *Phys. Rev. Lett.* **116** no. 20, (2016) 201301, [arXiv:1603.00464 \[astro-ph.CO\]](#).
- [24] M. Sasaki, T. Suyama, T. Tanaka, and S. Yokoyama, “Primordial Black Hole Scenario for the Gravitational-Wave Event GW150914,” *Phys. Rev. Lett.* **117** no. 6, (2016) 061101, [arXiv:1603.08338 \[astro-ph.CO\]](#).
- [25] Yu. N. Eroshenko, “Formation of PBHs binaries and gravitational waves from their merge,” [arXiv:1604.04932 \[astro-ph.CO\]](#).
- [26] S. Clesse and J. Garca-Bellido, “Detecting the gravitational wave background from primordial black hole dark matter,” [arXiv:1610.08479 \[astro-ph.CO\]](#).
- [27] B. Carr, F. Kuhnel, and M. Sandstad, “Primordial Black Holes as Dark Matter,” [arXiv:1607.06077 \[astro-ph.CO\]](#).
- [28] N. Orlofsky, A. Pierce, and J. D. Wells, “Inflationary theory and pulsar timing investigations of primordial black holes and gravitational waves,” *Phys. Rev. D* **95** no. 6, (2017) 063518, [arXiv:1612.05279 \[astro-ph.CO\]](#).
- [29] H. Nishikawa, E. D. Kovetz, M. Kamionkowski, and J. Silk, “Primordial-black-hole mergers in dark-matter spikes,” [arXiv:1708.08449 \[astro-ph.CO\]](#).
- [30] V. Takhistov, “Transmuted Gravity Wave Signals from Primordial Black Holes,” [arXiv:1707.05849 \[astro-ph.CO\]](#).
- [31] A. Klein *et al.*, “Science with the space-based interferometer eLISA: Supermassive black hole binaries,” *Phys. Rev. D* **93** no. 2, (2016) 024003, [arXiv:1511.05581 \[gr-qc\]](#).
- [32] S. Babak, J. Gair, A. Sesana, E. Barausse, C. F. Sopuerta, C. P. L. Berry, E. Berti, P. Amaro-Seoane, A. Petiteau, and A. Klein, “Science with the space-based interferometer LISA. V: Extreme mass-ratio inspirals,” [arXiv:1703.09722 \[gr-qc\]](#).
- [33] C. Hopman and T. Alexander, “The Orbital statistics of stellar inspiral and relaxation near a massive black hole: Characterizing gravitational wave sources,” *Astrophys. J.* **629** (2005) 362–372, [arXiv:astro-ph/0503672 \[astro-ph\]](#).
- [34] P. J. E. Peebles, “Star Distribution Near a Collapsed Object,” *apj* **178** (Dec., 1972) 371–376.
- [35] L. Ferrarese and D. Merritt, “A Fundamental relation between supermassive black holes and their host galaxies,” *Astrophys. J.* **539** (2000) L9, [arXiv:astro-ph/0006053 \[astro-ph\]](#).
- [36] K. Gebhardt *et al.*, “A Relationship between nuclear black hole mass and galaxy velocity dispersion,” *Astrophys. J.* **539** (2000) L13, [arXiv:astro-ph/0006289 \[astro-ph\]](#).
- [37] S. Tremaine *et al.*, “The slope of the black hole mass versus velocity dispersion correlation,” *Astrophys. J.* **574** (2002) 740–753, [arXiv:astro-ph/0203468 \[astro-ph\]](#).
- [38] J. Dubinski and R. G. Carlberg, “The Structure of cold dark matter halos,” *Astrophys. J.* **378** (1991) 496.
- [39] J. F. Navarro, C. S. Frenk, and S. D. M. White, “The Structure of cold dark matter halos,” *Astrophys. J.* **462** (1996) 563–575, [arXiv:astro-ph/9508025 \[astro-ph\]](#).
- [40] J. F. Navarro, C. S. Frenk, and S. D. M. White, “A Universal density profile from hierarchical clustering,” *Astrophys. J.* **490** (1997) 493–508, [arXiv:astro-ph/9611107 \[astro-ph\]](#).
- [41] B. Moore, T. R. Quinn, F. Governato, J. Stadel, and G. Lake, “Cold collapse and the core catastrophe,” *Mon. Not. Roy. Astron. Soc.* **310** (1999) 1147–1152, [arXiv:astro-ph/9903164 \[astro-ph\]](#).
- [42] S. Tulin and H.-B. Yu, “Dark Matter Self-interactions and Small Scale Structure,” [arXiv:1705.02358 \[hep-ph\]](#).
- [43] P. Gondolo and J. Silk, “Dark matter annihilation at the galactic center,” *Phys. Rev. Lett.* **83** (1999) 1719–1722, [arXiv:astro-ph/9906391 \[astro-ph\]](#).
- [44] L. Sadeghian, F. Ferrer, and C. M. Will, “Dark matter distributions around massive black holes: A general relativistic analysis,” *Phys. Rev. D* **88** no. 6, (2013) 063522, [arXiv:1305.2619 \[astro-ph.GA\]](#).
- [45] F. Ferrer, A. M. da Rosa, and C. M. Will, “Dark matter spikes in the vicinity of Kerr black holes,” [arXiv:1707.06302 \[astro-ph.CO\]](#).
- [46] A. A. Dutton and A. V. Macci, “Cold dark matter haloes in the Planck era: evolution of structural parameters for Einasto and NFW profiles,” *Mon. Not. Roy. Astron. Soc.* **441** no. 4, (2014) 3359–3374, [arXiv:1402.7073](#)

- [astro-ph.CO].
- [47] L. Ferrarese, “Beyond the bulge: a fundamental relation between supermassive black holes and dark matter halos,” *Astrophys. J.* **578** (2002) 90–97, [arXiv:astro-ph/0203469](#) [astro-ph].
- [48] J. R. Gair and K. Glampedakis, “Improved approximate inspirals of test-bodies into Kerr black holes,” *Phys. Rev. D* **73** (2006) 064037, [arXiv:gr-qc/0510129](#) [gr-qc].
- [49] S. Babak, H. Fang, J. R. Gair, K. Glampedakis, and S. A. Hughes, “‘Kludge’ gravitational waveforms for a test-body orbiting a Kerr black hole,” *Phys. Rev. D* **75** (2007) 024005, [arXiv:gr-qc/0607007](#) [gr-qc]. [Erratum: *Phys. Rev. D* **77**, 04990 (2008)].
- [50] P. C. Peters and J. Mathews, “Gravitational radiation from point masses in a Keplerian orbit,” *Phys. Rev.* **131** (1963) 435–439.
- [51] S. A. Teukolsky, “Perturbations of a rotating black hole. I. Fundamental equations for gravitational electromagnetic and neutrino field perturbations,” *Astrophys. J.* **185** (1973) 635–647.
- [52] M. Sasaki and T. Nakamura, “Gravitational Radiation From a Kerr Black Hole. 1. Formulation and a Method for Numerical Analysis,” *Prog. Theor. Phys.* **67** (1982) 1788.
- [53] L. S. Finn and K. S. Thorne, “Gravitational waves from a compact star in a circular, inspiral orbit, in the equatorial plane of a massive, spinning black hole, as observed by LISA,” *Phys. Rev. D* **62** (2000) 124021, [arXiv:gr-qc/0007074](#) [gr-qc].
- [54] J. R. Gair, “Probing black holes at low redshift using LISA EMRI observations,” *Class. Quant. Grav.* **26** (2009) 094034, [arXiv:0811.0188](#) [gr-qc].
- [55] J. M. Bardeen, W. H. Press, and S. A. Teukolsky, “Rotating black holes: Locally nonrotating frames, energy extraction, and scalar synchrotron radiation,” *Astrophys. J.* **178** (1972) 347.
- [56] H. Kudoh, A. Taruya, T. Hiramatsu, and Y. Himemoto, “Detecting a gravitational-wave background with next-generation space interferometers,” *Phys. Rev. D* **73** (2006) 064006, [arXiv:gr-qc/0511145](#) [gr-qc].
- [57] K. C.W. Misner and J.A. Wheeler, *Gravitation*. Freeman, San Francisco, 1973.
- [58] C. Hopman and T. Alexander, “Resonant relaxation near a massive black hole: the stellar distribution and gravitational wave sources,” *Astrophys. J.* **645** (2006) 1152–1163, [arXiv:astro-ph/0601161](#) [astro-ph].
- [59] C. Hopman and T. Alexander, “The effect of mass-segregation on gravitational wave sources near massive black holes,” *Astrophys. J.* **645** (2006) L133–L136, [arXiv:astro-ph/0603324](#) [astro-ph].
- [60] C. Hopman, “Extreme mass ratio inspiral rates: dependence on the massive black hole mass,” *Class. Quant. Grav.* **26** (2009) 094028, [arXiv:0901.1667](#) [astro-ph].
- [61] J. Miralda-Escude and A. Gould, “A cluster of black holes at the galactic center,” *Astrophys. J.* **545** (2000) 847, [arXiv:astro-ph/0003269](#) [astro-ph].
- [62] P. Amaro-Seoane and M. Preto, “The impact of realistic models of mass segregation on the event rate of extreme-mass ratio inspirals and cusp re-growth,” *Class. Quant. Grav.* **28** (2011) 094017, [arXiv:1010.5781](#) [astro-ph.CO].
- [63] T. Alexander and C. Hopman, “Strong mass segregation around a massive black hole,” *Astrophys. J.* **697** (2009) 1861–1869, [arXiv:0808.3150](#) [astro-ph].
- [64] M. Preto and P. Amaro-Seoane, “On strong mass segregation around a massive black hole: Implications for lower-frequency gravitational-wave astrophysics,” *Astrophys. J.* **708** (2010) L42, [arXiv:0910.3206](#) [astro-ph.GA].
- [65] K. Belczynski, T. Bulik, C. L. Fryer, A. Ruitter, J. S. Vink, and J. R. Hurley, “On The Maximum Mass of Stellar Black Holes,” *Astrophys. J.* **714** (2010) 1217–1226, [arXiv:0904.2784](#) [astro-ph.SR].
- [66] J. Georg and S. Watson, “A Preferred Mass Range for Primordial Black Hole Formation and Black Holes as Dark Matter Revisited,” [arXiv:1703.04825](#) [astro-ph.CO].
- [67] B. Kiziltan, A. Kottas, M. De Yoreo, and S. E. Thorsett, “The Neutron Star Mass Distribution,” *Astrophys. J.* **778** (2013) 66, [arXiv:1309.6635](#) [astro-ph.SR].
- [68] S. O. Kepler, D. Koester, A. D. Romero, G. Ourique, and I. Pelisoli, “White Dwarf Mass Distribution,” in *20th European White Dwarf Workshop*, P.-E. Tremblay, B. Gaensicke, and T. Marsh, eds., vol. 509 of *Astronomical Society of the Pacific Conference Series*, p. 421. Mar., 2017. [arXiv:1610.00371](#) [astro-ph.SR].
- [69] C. Caprini *et al.*, “Science with the space-based interferometer eLISA. II: Gravitational waves from cosmological phase transitions,” *JCAP* **1604** no. 04, (2016) 001, [arXiv:1512.06239](#) [astro-ph.CO].
- [70] A. Petiteau, G. Auger, H. Halloin, O. Jeannin, E. Plagnol, S. Pireaux, T. Regimbau, and J.-Y. Vinet, “LISACode: A Scientific simulator of LISA,” *Phys. Rev. D* **77** (2008) 023002, [arXiv:0802.2023](#) [gr-qc].
- [71] F. Khnel, G. D. Starkman, and K. Freese, “Primordial Black-Hole and Macroscopic Dark-Matter Constraints with LISA,” [arXiv:1705.10361](#) [gr-qc].
- [72] We note that the sensitivity curves LISA-C1 and LISA-C4, taken from Ref. [69], are obtained from LISACode [70]. They are slightly different from the LISA sensitivity presented in Ref. [19].
- [73] Using LISA to detect the GW radiation from PBH inspiraling into Sagittarius A* is also discussed in [71]. This paper considers the GW emission before merging, which is the stochastic signal from the extreme long time ongoing inspirals. However, as we will discuss later, the scatterings between PBH and other stellar objects can easily change PBH’s orbit, which is crucial for the events counting. Neglecting them will largely overestimate the event rate. Further the GW frequency distribution spans a large range and needs to be studied more carefully in order to properly calculate SNR.
- [74] For simplicity, we assume PBH and MS share the same power law, i.e. p , as spatial distribution. This is reasonable when PBH is lighter or comparable to $\mathcal{O}(1) M_{\odot}$. It is not difficult to derive a similar formula with different choices on p .